Bosons with multifractal energy spectrum: specific heat log periodicity and Bose–Einstein condensation

2005 J. Phys.: Condens. Matter 17 3499

(http://iopscience.iop.org/0953-8984/17/23/003)

INSTITUTE OF PHYSICS PUBLISHING JOURNAL OF PHYSICS: CONDENSED MATTER

J. Phys.: Condens. Matter **17** (2005) 3499–3508 doi:10.1088/0953-8984/17/23/003

Bosons with multifractal energy spectrum: specific heat log periodicity and Bose–Einstein condensation

I N de Oliveira[1], M L Lyra[1], E L Albuquerque[2] and L R da Silva[2]

[1] Departamento de Física, Universidade Federal de Alagoas, 57072-970 Maceió-AL, Brazil
[2] Departamento de Física, Universidade Federal do Rio Grande do Norte, 59072-970 Natal-RN, Brazil

E-mail: marcelo@df.ufal.br

Received 28 February 2005, in final form 5 April 2005
Published 27 May 2005
Online at stacks.iop.org/JPhysCM/17/3499

Abstract

The thermodynamics for systems of non-interacting bosons with multifractal energy spectrum is considered. The critical attractors of one-dimensional generalized logistic and circular maps are used to generate multifractal bounded spectra with well defined scaling exponents. The specific heat is then calculated for both cases of conserved and non-conserved particle number, showing a power-law behaviour which is modulated by log-periodic oscillations when the energy spectrum is not dense. The occurrence of Bose–Einstein condensation for systems with conserved particle number, at which the specific heat is discontinuous, is also analyzed.

1. Introduction

The existence of quasicrystals was first inferred from the experimental observation of sharp diffraction patterns with a symmetry forbidden in periodic lattices [1], producing a great interest in the understanding of the properties of these system. They lack translational symmetry but, unlike disordered lattices, display long-range order. Besides, their optical patterns are consistent with aperiodic geometry, having properties that are intermediate between periodic structures (Bloch systems) and random materials, in spite of the purely deterministic rules used to generate them [2, 3].

It is well known that the term *quasicrystal* is more appropriate for natural compounds or artificial alloys, although in one dimension there is no difference between this and the quasiperiodic structure formed by the incommensurate arrangement of periodic unit cells (for a review see [4]). An appealing motivation, and perhaps the most characteristic one, for studying such structures is that they exhibit a highly fragmented energy spectrum displaying a self-similar pattern. Indeed, from a strictly mathematical perspective, it has been proven that their spectra are *Cantor sets* in the thermodynamic limit [5–7]. These spectra, however, tend to be very complex, and simplified fractal models have been used to explain their properties.

Simplified fractals based on the Cantor set and Fibonacci sequence [8–11], as well as the critical attractor of the logistic and circular maps at the onset of chaos [12–14], have been used recently to model the energy spectrum of quasiperiodic systems. The thermodynamic behaviour derived from such self-similar spectra displays some anomalous features, the most prominent one being related to the emergence of log-periodic oscillations in the low-temperature behaviour of the specific heat. The origin of these oscillations can be directly identified as the longest wavelength oscillations on the integrated density of states (IDOS) when it is expressed in terms of the logarithm of the energy. Furthermore, a series of recent works looking for connections with the quasiperiodic aspects of these spectra (scaling laws, fractal dimension, etc) as well as for some kind of common behaviour in the specific heat spectra has shown, among other things, that the low-temperature log-periodicity of the specific heat is intimately connected with some underlying fractal dimension characterizing the energy spectrum [15–17]. Log-periodic oscillations have been observed to appear in general natural systems with some underlying discrete scale invariance [18, 19].

In this work, we intend to extend the study of the thermodynamic properties of systems with multifractal energy spectra, by considering that the quasi-particles obey the Bose–Einstein quantum statistics. Both cases of conserved and non-conserved particle number will be treated. Systems with conserved number of particles, for example gases of massive particles, have a non-null chemical potential. Therefore, the particles may condense in the ground state at low temperatures through a Bose–Einstein transition, for example the normal to superconductor transition which occurs due to the condensation of Cooper pairs. The proximity effect of a superconductor to a normal system with fractal spectrum has been recently investigated [20]. We will also study the case of non-conserved particle number which describes the thermodynamic associated with collective excitations. However, we will restrict our study to bounded energy spectra, which is more likely to represent phonon energy spectra. Although the spectra of quasicrystalline materials are generally used to account for electronic properties, the phonon spectra have also been studied [21–24]. Scattering processes involving phonons are fundamental to understand some features of the low-temperature thermal [25] as well as electrical [26] conductivity of quasicrystals. In what follows, the energy spectra are derived from the critical attractors of the families of logistic and circular maps which, at the onset of chaos, exhibit a multifractal structure with long-range temporal and spatial correlations. We are particularly interested in identify the relationship between the scaling exponents characterizing the multifractal energy spectra and the resulting thermodynamic behaviour. Our purpose is twofold: on the one hand, we will show that the emergence of the log-periodic oscillations of the specific heat is directly connected with both the fractal dimension of the energy scale support and the singularity strength associated with one member of the extremal set of the multifractal attractor. On the other hand, we discuss the occurrence of a Bose–Einstein condensation linked to the scaling behaviour of the energy spectrum.

This paper is structured as follows: we present in section 2 our theoretical model to generate the multifractal energy spectrum for both the logistic and the circular maps. Then we proceed to show in section 3 the specific heat profile associated with their energy spectrum. Special attention is devoted to the Bose–Einstein condensation which depends on the integrated density of states scaling at the bottom of the band. Finally, the conclusions of this work are presented in section 4.

2. Energy spectrum

Logistic-like maps represent a class of simple dynamical systems where the production of chaos can be observed. In their generalized form, this family is represented by

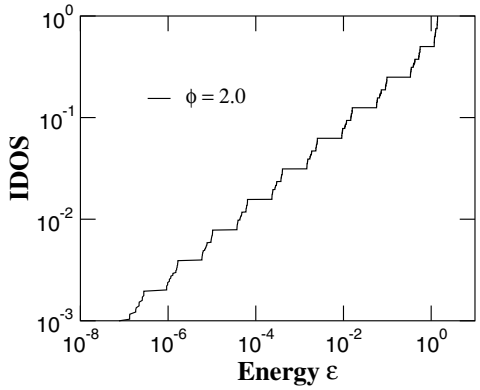

Figure 1. Integrated density of states (IDOS) as a function of energy ε for the logistic-like map at the onset of chaos defined by equation (1), considering the exponent $\phi = 2.0$.

$$x_{i+1} = 1 - a|x_i|^{\phi}, \tag{1}$$

where the exponent ϕ is the inflexion of the map in the neighbourhood of the extremal point $\bar{x} = 0$. This family of maps displays topological properties which are not dependent on the exponent ϕ. Although metrical properties, such as the support fractal dimension and Feigenbaum's exponents, depend on ϕ, the attractors exhibit cascades of bifurcations converging at a critical point $a_c(\phi)$ for all values of $\phi > 1$.

Another example of dynamical systems where chaotic orbits can be observed is composed of the family of circular-like maps defined as

$$\theta_{i+1} = \Omega + [\theta_i - (K/2\pi)\sin(2\pi\theta_i)]^{\phi/3}, \tag{2}$$

with $0 < \Omega < 1$ and $0 < K < \infty$. For $K = 1$ these maps present critical orbits for which the renormalized winding number $\omega = \lim_{t\to 0}(\theta_{t+1} - \theta_t)$ is equal to the Fibonacci golden mean $\tau = (1 + \sqrt{5})/2$ [27].

These two families of maps exhibit a transition to chaos via quasiperiodicity. However, they have distinct scaling behaviours for the same value of ϕ, belonging to different universality classes. At the critical point, the dynamical attractor can be characterized by a multifractal measure [28]. The multifractal behaviour can be described by the spectrum of the scaling indices $f(\alpha)$ which expresses the dimensions of each subset with singularity strength α. The continuous function $f(\alpha)$ has a parabolic-like shape within the range $[\alpha_{\min}, \alpha_{\max}]$, where the maximum value $f(\alpha_0)$ is the support's fractal dimension d_f. The singularity strengths $\alpha_{\min}$ and $\alpha_{\max}$ are associated, respectively, with the regions where the measure is most concentrated and most rarefied. Both the circular-like maps and the logistic-like maps have been extensively studied and their attractor properties at the critical point are well known for distinct values of ϕ [29].

In what follows, the energy spectrum is associated with the critical attractor of both the logistic-like and the circular-like maps for specific values of ϕ. We associate each point of the attractor with a dimensionless energy ε_i. Thus, these maps generate a multifractal energy spectrum which can be used to investigate the thermal properties of systems with quasiperiodic structures. Figure 1 depicts the integrated density of states (IDOS) as a function of energy for the logistic map at the onset of chaos with $\phi = 2.0$, considering a dimensionless energy spectrum given by

$$\varepsilon_i = \frac{x_i - \min[x_i]}{\max[x_i] - \min[x_i]}. \tag{3}$$

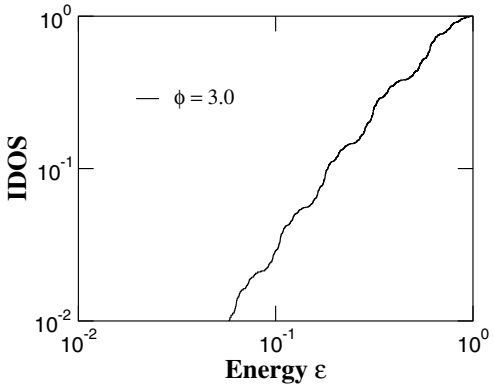

Figure 2. The same as in figure 1, but for the circular-like map defined by equation (2), considering the exponent $\phi = 3.0$.

The staircase aspect of IDOS reveals the discrete scale invariance of the spectrum. Also, we can verify that IDOS has a fragmented structure at the bottom of the band which results from the fact that the attractor is not dense with fractal dimension $d_f < 1$. In figure 2 we present the integrated density of states for the circular map with $\phi = 3.0$. In this case, the dimensionless energy is given by $\varepsilon_i = \theta_i$. We can notice again the scale invariance of the spectrum. However, there are no gaps in the band because the attractor is dense with the fractal dimension $d_f = 1$.

The IDOS scaling at the bottom of the band determines the low-temperature properties of systems with quasiperiodic structures. For both families of maps, we are particularly interested in computing the specific heat using Bose–Einstein statistics with either conserved or non-conserved number of particles. For the logistic-like maps, we generated $N = 2^{14} = 16\,384$ points in the attractor while for the circular-like maps the number of points in the attractor corresponds to the Fibonacci number $F_{20} = 17\,711$.

The presence of long range correlations in this and other systems avoids canonical approaches like perturbation theory, where one first separates a small localized piece of the system, treating the rest as perturbation *a posteriori*. This approach does not work in those cases, because the behaviour of the macroscopic system is completely distinct of the behaviour of its separated small piece, due to the long range correlations. Fortunately, the presence of long range correlations itself gives the key to circumvent this difficulty: normally these systems are very robust to wide modifications on a microscopic scale. In the study of continuous phase transitions, for instance, the critical behaviour is known to depend only upon global properties, namely the geometric dimension of the system and the symmetries of its order parameter, being insensitive to the details of the microscopic interactions between atoms or molecules. A striking example is the Ising model used to describe water: the molecules are simply replaced by classical spins *up* diluted on a lattice, sites with spin *down* corresponding to the absence of a molecule there [30, 31]. Also, the complicated interactions between these molecules are replaced by a simple nearest-neighbour coupling constant. In spite of its simplicity, this model reproduces quite well the behaviour of water near its critical temperature. The important consequence of this robustness, i.e., many systems which are distinct within a microscopic scale presenting the same critical behaviour, is that one can thus classify the various systems in a few *universality classes*. Further, it is worthy of mention here that the finite sampling sizes we will consider in the following study of the thermodynamics properties are large enough to achieve the scaling behaviour of the multifractal spectrum. The reported results remained

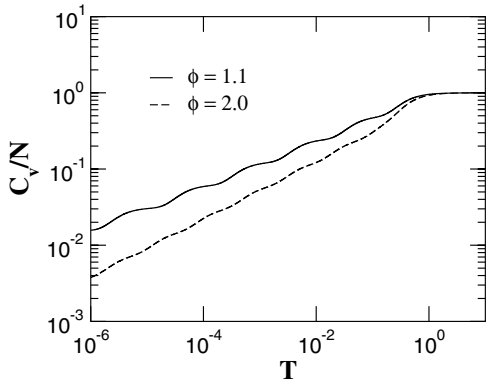

Figure 3. The normalized specific heat as a function of temperature for energy spectra generated from critical points of logistic-like maps. We considered two distinct values of ϕ, namely $\phi = 1.1$ (solid line) and 2.0 (dashed line). Notice the oscillatory behaviour around a power law decay at low temperatures $C_V \propto T^{\alpha_{\min}}$.

fairly much the same when we used longer samplings except by small corrections at very low temperatures and at the vicinity of the Bose–Einstein condensation, at which we employ a finite-size scaling analysis to characterize its nature.

3. Specific heat

Now we use the multifractal energy spectrum, as described in the last section, to determine the specific heat. Many of the general statistical mechanics results we will refer to can be found in [32]. First we compute the specific heat for a system with unconstrained particle number. In this case, the chemical potential μ is null. As the energy spectrum is bounded, the thermodynamics derived will resemble that of phonons which have a finite specific heat at high temperatures. From Bose–Einstein statistics, the average occupation number for each energy state is given by

$$\langle n_i \rangle = \frac{1}{[\exp(\beta\varepsilon_i) - 1]}, \tag{4}$$

where $\beta = 1/k_{\mathrm{B}}T$ (in what follows we will use units of $k_{\mathrm{B}} = 1$). The average internal energy can be computed from

$$U(N, T) = \sum_{i=1}^{N} \varepsilon_i \langle n_i \rangle. \tag{5}$$

The specific heat is evaluated by differentiating the average internal energy $U(N, T)$ with respect to the temperature T, i.e., $C_v = \mathrm{d}U(N, T)/\mathrm{d}T|_V$, where V is the volume of the system, which is kept constant by maintaining fixed the total number of one-particle accessible states N. From equation (5), we compute the specific heat as

$$C_v = (1/2T)^2 \left[\sum_i \varepsilon_i^2 \sinh^{-2}(\varepsilon_i/2T) \right]. \tag{6}$$

In figure 3, we plot the normalized specific heat as a function of temperature for two distinct values of ϕ, namely $\phi = 1.1$ (solid line) and 2.0 (dashed line), using the critical attractor points of the logistic-like maps to generate the multifractal energy spectra. In both cases, we observe

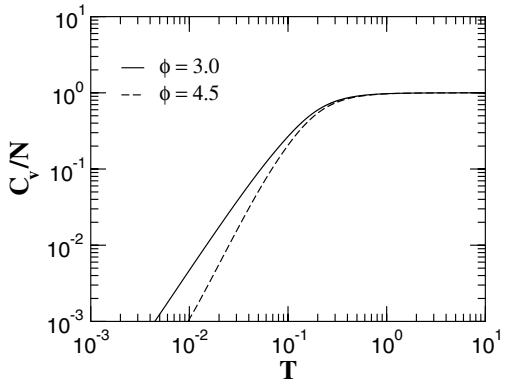

Figure 4. Log–log plot of the normalized specific heat as a function of temperature for the energy spectra derived from circular-like maps, considering $\phi = 3.0$ (solid line) and 4.5 (dashed line). The specific heat presents a power-law decay at low temperatures as $C_V \propto T^{\alpha_{\max}}$.

that the specific heat displays a non-linear vanishing of the form $C_v/N \propto T^{\eta}$, where the exponent η is equal to the minimum singularity strength $\alpha_{\min}$. This exponent is the same as displayed by the IDOS near the bottom of the band. Also, we can notice that the specific heat presents log-periodic oscillations resulting from the hierarchical band gaps. The number of particles vanishes as $T \to 0$. On the other hand, as the temperature increases, particles are generated which can occupy energy states at different scales, which explains the specific heat oscillations. In the high temperature regime, the specific heat saturates at a $C_V/N = 1$. The saturation of C_V/N is a general feature of systems with non-conserved particle number and bounded energy spectrum.

The amplitude of the specific heat oscillations is directly related to the support fractal dimension. For logistic-like maps, the attractor is not dense ($d_{\rm f} < 1$) and the fractal dimension increases with the map inflexion, thus resulting in smaller oscillation amplitudes for larger non-linearities. On the other hand, for dense energy spectra ($d_{\rm f} = 1$), we can anticipate that the specific heat will not present log periodic oscillations. This can be corroborated by computing the specific heat as a function of temperature using energy spectra generated from the attractor of circular-like maps for different values of ϕ, namely $\phi = 3.0$ (solid line) and 4.5 (dashed line), as shown in figure 4. For the circular-like maps, the support fractal dimension of the dynamical attractor is exactly $d_{\rm f} = 1$. In this case, the specific heat presents a power-law decay in the region of low temperatures but does not present log-periodic oscillations. The power-law exponent is equal to the maximum singularity spectrum once the most rarefied set of the multifractal attractor governs the main scaling behaviour at the bottom of the energy band.

Next, we will consider systems in which the number of bosons is conserved, as in gases of massive particles. In this case both low- and high-temperature behaviours are strongly affected by the constraint in the particle number. At low temperatures the particles may condensate at the ground state instead of just disappear as happens with collective excitations. At high temperatures the internal energy saturates once new particles cannot be created and the specific heat vanishes as $T \to \infty$. Considering the grand canonical ensemble, the average number of particles at the ith energy state is defined by

$$\langle n_i \rangle = \frac{1}{z^{-1}\exp(\beta\varepsilon_i) - 1}. \tag{7}$$

Here $z = \exp(\beta\mu)$ is the fugacity, where μ is the chemical potential which can be extracted

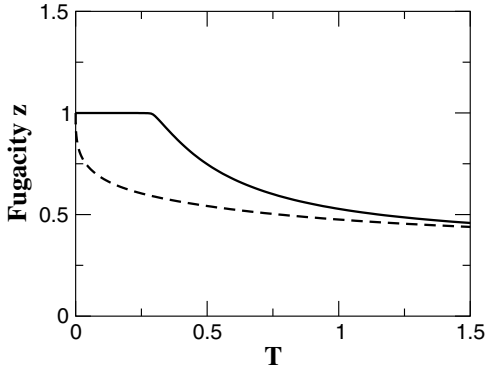

Figure 5. The fugacity as a function of temperature for energy spectra generated from the circular-like map (solid line) and the logistic-like map (dashed line). The map inflexions are $\phi = 3.0$ (solid line) and $\phi = 1.1$ (dashed line).

from

$$N_{\rm p} = \sum_{i=1}^{N} \langle n_i \rangle, \tag{8}$$

where $N_{\rm p}$ is the number of conserved boson particles. In what follows, we will use $N_{\rm p} = N/2$. In figure 5, we show the fugacity dependence on temperature for the energy spectra generated from critical attractor points of logistic and circular maps. Again, we can notice a great difference among the thermal properties of these systems. For the logistic map (dashed line in figure 5), we can observe that the fugacity presents a monotonic decay as the temperature increases. For the circular map (solid line in figure 5), the fugacity assumes values near unity at low temperatures, presenting a monotonic decay afterwards. This indicates that a macroscopic fraction of particles is in a single energy state $\varepsilon_i = 0$, i.e., this system displays a *Bose–Einstein condensation* at low temperatures. The existence of a Bose–Einstein condensation depends on the IDOS scale at the bottom of the band. For energy spectra derived from the generalized logistic maps, the IDOS scales with $\varepsilon_i^{\alpha_{\rm min}}$. As $\alpha_{\rm min} < 1$, a Bose–Einstein condensation cannot be reached. Using the circular-like maps to generate the energy spectra, the IDOS scales as $\varepsilon_i^{\alpha_{\rm max}}$. As in this case $\alpha_{\rm max} > 1$, the IDOS increases faster than linearly and a Bose–Einstein condensation takes place.

The number of particles at the ground state, namely N_0, is related to the fugacity as $N_0 = z/(1-z)$. In figure 6, we plot the fraction of particles at the ground state $N_0/N_{\rm p}$ as a function of temperature for two inflexion points of the circular map, namely $\phi = 3.0$ (solid line) and $\phi = 4.5$ (dashed line), respectively. For low temperatures, the fraction $N_0/N_{\rm p}$ is finite, vanishing at a finite temperature which depends on the inflexion point. We assume this temperature to be the transition temperature $T_{\rm c}$. The transition temperature becomes higher for larger inflexion points, as it is shown in figure 7.

Using equation (5), with the help of equation (6) we can derive the specific heat as

$$4T^2 C_v = \sum_i \varepsilon_i^2 \sinh^{-2}(y_i) - \left[\sum_i \varepsilon_i \sinh^{-2}(y_i)\right]^2 \Big/ \sum_i \sinh^{-2}(y_i), \tag{9}$$

with $y_i = (\varepsilon_i - \mu)/2T$.

In figure 8, we show the specific heat as a function of temperature for conserved bosons and a dense spectrum derived from generalized circular maps. We have considered $\phi = 3.0$ (solid line) and 4.5 (dashed line). We can notice that the specific heat has a discontinuity at $T = T_{\rm c}$,

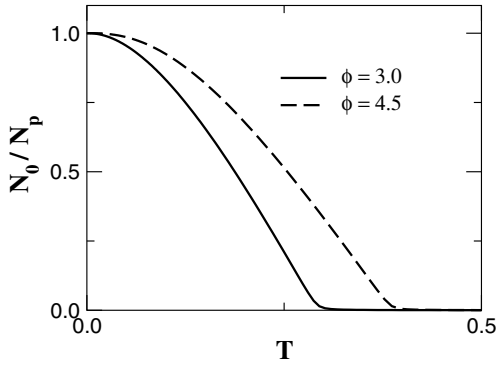

Figure 6. Fraction of particles N_0/N_p in the ground state as a function of temperature considering $\phi = 3.0$ (solid line) and $\phi = 4.5$ (dashed line). The condensed fraction vanishes at a transition temperature which increases with ϕ.

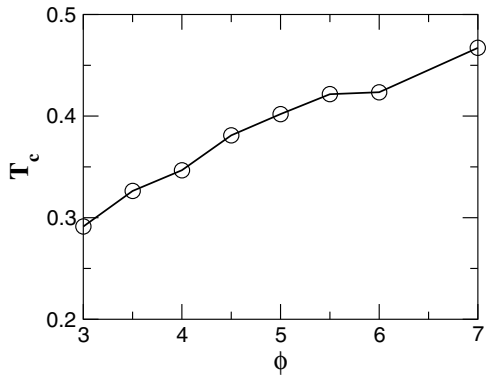

Figure 7. The Bose–Einstein condensation transition temperature as a function of ϕ for energy spectra derived from the generalized circular maps.

which is more evident as the exponent ϕ increases. For the finite number of energy states used the discontinuity is rounded. We have computed the specific heat considering distinct number of states N (distinct generations of the underlying multifractal spectra). They provide similar figures with a crossing point at the transition temperature, confirming the specific heat discontinuity in the limit of $N \to \infty$. In this case, no evident low-temperature oscillations are depicted. In figure 9, we show the corresponding result obtained by using the logistic attractor considering $\phi = 1.1$ (solid line) and 2.0 (dashed line). Similar to the case of non-conserved particle number, the specific heat presents an oscillatory non-linear decay at low temperatures but no Bose–Einstein condensation. At high temperatures the specific heat vanishes as T^{-2}, which is typical of systems with conserved particle number and bounded energy spectrum.

4. Conclusions

We have considered in this study a detailed analysis of the thermodynamic behaviour of systems with non-interacting bosons exhibiting multifractal energy spectra derived from the critical attractor of iterated maps, namely the logistic and circular-like maps. The main purpose of using multifractal measures derived from dynamical systems was based on the fact that their

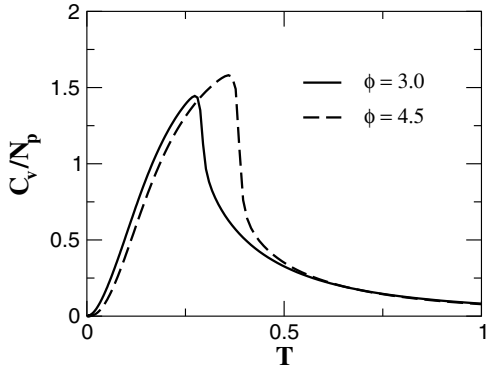

Figure 8. The normalized specific heat for conserved particle number as a function of temperature for energy spectra obtained from the circular-like maps at the onset of chaos. We have considered $\phi = 3.0$ (solid line) and 4.5 (dashed line). We can observe that the specific heat has a discontinuity at the transition temperature. At high temperatures the specific heat vanishes as T^{-2}, which is typical of systems with conserved particle number and bounded energy spectrum.

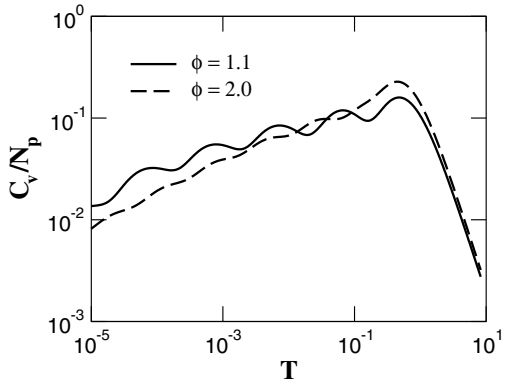

Figure 9. Log–log plot of the normalized specific heat as a function of temperature and conserved particle number for $\phi = 1.1$ (solid line) and 2.0 (dashed line). The energy spectra were obtained from critical attractor points of the logistic-like maps. No Bose–Einstein condensation is present.

scaling behaviour can be deeply understood and tuned by varying model parameters such as the kind of non-linearity. Therefore, they represent an important tool to study in detail the relationship between specific scaling features of the underlying multifractal spectrum and the thermodynamic properties.

For systems with non-conserved particle number, the specific heat was shown to exhibit a power-law behaviour at low temperatures. The vanishing of the specific heat is governed by the scaling exponent characterizing the growth of the integrated density of states at the bottom of the energy band. For instance, for the logistic-like maps this exponent is the singularity strength of the most concentrated sets of the multifractal spectra $\alpha_{\min}$. On the other hand, the circular-like maps have the most rarefied sets at the bottom of the band and the specific heat vanishing exponent is the maximum singularity strength $\alpha_{\max}$. The power-law low-temperature behaviour was observed to be modulated by log-periodic oscillations whenever the energy spectrum has fractal dimension $d_f < 1$, as is the case of the logistic maps. At high temperatures, the specific heat saturates at a constant value.

On the other hand, for systems with conserved particle number the low-temperature behaviour was shown to be similar. At high temperatures, the specific heat displays the typical T^{-2} decay. Furthermore, as the chemical potential μ is non-null, a Bose–Einstein condensation, which depends on the integrated density of states scale at the bottom of the band, may take place. For the logistic maps the IDOS increases more slowly than linearly and, therefore, there is no Bose–Einstein condensation. However, the large values of $\alpha_{\max} > 1$ for the circular maps provide the necessary condition for this transition to occur. The specific heat is discontinuous at the Bose–Einstein condensation transition, whose temperature increases monotonically with the map non-linearity. The above trends are quite general for non-interacting bosons and will be taken into account when analysing the thermodynamic behaviour associated with bosonic systems with scale invariant energy spectra.

Acknowledgments

We would like to thank CAPES-Procad, CNPq, MCT-NanoSemiMat, and FINEP-CTInfra (Brazilian Research Agencies) as well as FAPEAL (Alagoas State Research Agency) for partial financial support.

References

[1] Schechtman D, Blech I, Gratias D and Cahn J W 1984 *Phys. Rev. Lett.* **53** 1951
[2] Levine D and Steinhardt P J 1984 *Phys. Rev. Lett.* **53** 2477
[3] Senechal M 1995 *Quasicrystals and Geometry* (Cambridge: Cambridge University Press)
[4] Albuquerque E L and Cottam M G 2003 *Phys. Rep.* **376** 225
[5] Süto A 1989 *J. Stat. Phys.* **56** 525
[6] Bellisard J, Bovier A and Ghez J-M 1991 *Commun. Math. Phys.* **135** 379
[7] Bovier A and Ghez J-M 1993 *Commun. Math. Phys.* **158** 45
[8] Tsallis C, da Silva L R, Mendes R S, Vallejos R O and Mariz A M 1997 *Phys. Rev.* E **56** R4922
[9] Vallejos R O, Mendes R S, da Silva L R and Tsallis C 1998 *Phys. Rev.* E **58** 1346
[10] Vallejos R O and Anteneodo C 1998 *Phys. Rev.* E **58** 4134
[11] Carpena P, Coronado A V and Galván P B 2000 *Phys. Rev.* E **61** 2281
[12] Peitgen H-O, Jurgens H and Saupe D 1992 *Chaos and Fractals* (Heidelberg: Springer)
[13] da Silva L R, Vallejos R O, Tsallis C, Mendes R S and Roux S 2001 *Phys. Rev.* E **64** 11104
[14] de Oliveira I N, Lyra M L and Albuqurque E L 2004 *Physica* A **343** 424
[15] Mauriz P W, Albuquerque E L and Vasconcelos M S 2001 *Phys. Rev.* B **63** 184203
[16] Bezerra C G, Albuquerque E L, Mariz A M, da Silva L R and Tsallis C 2001 *Physica* A **294** 415
[17] Mauriz P W, Vasconcelos M S and Albuquerque E L 2003 *Physica* A **329** 101
[18] Sornette D 1998 *Phys. Rep.* **295** 239
[19] Roy A, Roy S, Bhattacharyya A J, Banerjee S and Tarafdar S 1999 *Eur. Phys. J.* B **12** 1
[20] Ossipov A and Kottos T 2004 *Phys. Rev. Lett.* **92** 017004
[21] Socolar J E S, Lubenski T C and Steinhardt P J 1986 *Phys. Rev.* B **34** 3345
[22] Krajci M and Hafner J 1993 *J. Non-Cryst. Solids* **156** 887
[23] Quilichini M and Janssen T 1997 *Rev. Mod. Phys.* **69** 277
[24] Anselmo D H A L, Dantas A L, Medeiros S K, Albuquerque E L and Freire V N 2005 *Physica* A **349** 259
[25] Gianno K, Sologubenko A V, Chernikov M A, Ott H R, Fisher I R and Canfield P C 2000 *Phys. Rev.* B **62** 292
[26] Azhazha V, Khadzhay G, Malikhin S, Merisov B and Pugachov A 2003 *Phys. Lett.* A **319** 539
[27] Jensen M H, Kadanoff L P, Libchaber A, Procaccia I and Stavans J 1985 *Phys. Rev. Lett.* **55** 2798
[28] Strogatz S H 1994 *Nonlinear Dynamics and Chaos* (Reading, MA: Addison-Wesley)
[29] da Silva C R, da Cruz H R and Lyra M L 1999 *Braz. J. Phys.* **29** 144
[30] Sartorelli J C, Gonçalves W M and Pinto R D 1994 *Phys. Rev.* B **49** 3963
[31] Penna T J P, de Oliveira P M C, Sartorelli J C, Gonçalves W M and Pinto R D 1995 *Phys. Rev.* E **52** R2168
[32] Reichl L E 1998 *A Modern Course in Statistical Physics* (New York: Wiley)